Supplementary Information

Morphology shapes microbial ecosystems and carbon cycling within cryoconite holes on a Greenland outlet glacier

Nozomu Takeuchi[1], Takumi Murakami[2], Koki Ishiwatari[1], Akane Watanabe[1], Takahiro Segawa[3]

1 Department of Earth Sciences, Graduate School of Science, Chiba University, Chiba 263-8522, Japan.

2 School of Life Science and Technology, Institute of Science Tokyo, 2-12-1 Ookayama, Meguro-ku, Tokyo 152-8550 Japan

3 Center for Life Science Research, University of Yamanashi, 1110, Shimokato, Chuo, Yamanashi 400-0016, Japan

Correspondence to: Nozomu Takeuchi (ntakeuch@faculty.chiba-u.jp)

This PDF file includes:

Supplementary Table S1-S2

Supplementary Figures S1–S5

Table S1: Location and dimensions of cryoconite holes at 20 study sites on Issunguata Sermia in southwest Greenland. (SD represents standard deviation)

Site	Latitude	Longitude	Elevation	Number of holes measured	Diameter (mean±SD)	Depth (mean±SD)	Water level (mean±SD)
	degree	degree	m a.s.l.	holes	cm	cm	cm
S1	67.162185	-50.039245	492	-	-	-	-
S2	67.164011	-50.038652	523	5	2.8 ± 0.45	4.6 ± 0.55	2.6 ± 1.14
S3	67.165815	-50.039734	531	10	2.5 ± 0.71	6.7 ± 1.57	4.4 ± 2.17
S4	67.167680	-50.039809	537	10	3.8 ± 1.62	8.2 ± 0.79	7.4 ± 1.35
S5	67.169524	-50.039565	555	10	3.4 ± 0.84	12.4 ± 2.41	7.3 ± 1.06
S6	67.171341	-50.038944	559	10	3.4 ± 1.43	7.3 ± 2.21	3.6 ± 1.96
S7	67.172872	-50.036396	573	10	3.6 ± 0.70	16.9 ± 3.28	14.6 ± 3.24
S8	67.174498	-50.034090	573	10	2.9 ± 0.57	10.6 ± 1.43	8.3 ± 1.70
S9	67.176150	-50.031907	577	10	3.4 ± 0.84	14.6 ± 1.43	9.7 ± 1.77
S10	67.177938	-50.030019	573	10	3.1 ± 1.10	11.6 ± 1.71	5.4 ± 0.84
S11	67.179561	-50.028219	573	10	4.0 ± 1.33	15.4 ± 3.37	5.0 ± 2.31
S12	67.181284	-50.026438	574	10	3.6 ± 1.51	12.6 ± 3.44	7.2 ± 3.55
S13	67.182963	-50.024222	579	10	6.8 ± 2.53	24.5 ± 3.06	19.3 ± 2.98
S14	67.184613	-50.021917	582	10	7.2 ± 2.25	20.6 ± 1.58	17.8 ± 1.87
S15	67.186285	-50.020156	588	10	5.3 ± 1.64	23.8 ± 3.49	18.1 ± 2.47
S16	67.187969	-50.018480	585	10	3.5 ± 0.97	19.2 ± 1.62	13.3 ± 3.40
S17	67.189751	-50.017221	584	10	4.5 ± 0.97	20.5 ± 1.43	14.1 ± 2.92
S18	67.191579	-50.017216	586	10	4.8 ± 1.48	22.2 ± 3.36	17.1 ± 2.08
S19	67.193436	-50.017763	588	10	4.8 ± 1.75	20.3 ± 1.57	15.6 ± 1.26
S20	67.195290	-50.018214	587	10	4.8 ± 1.48	24.4 ± 2.22	20.4 ± 2.88
Mean					4.1	15.6	11.1
S.D.					1.3	6.4	5.9

Table S2: Geochemical data for cryoconite and meltwater from cryoconite holes on Issunguata Sermia Glacier in southwest Greenland.

Site	Cryoconite						Meltwater											
	OM	N	C	C/N	$\delta^{15}N$	$\delta^{13}C$	$\delta^{18}O$	δD	Cl^-	NO_2^-	NO_3^-	PO_4^{3-}	SO_4^{2-}	Na^+	NH_4^+	K^+	Mg^{2+}	Ca^{2+}
	w%	w%	w%	w/w	‰	‰	‰	‰	ppb	ppb	ppb	ppb	ppb	ppb	ppb	ppb	ppb	ppb
S1	1.7	0.1	0.7	8.2	-1.1	-20.2	-26.7	-211	25.8	0.0	11.3	0.0	18.8	17.7	0.0	67.3	24.4	68.2
S2	1.4	0.1	0.6	9.5	-1.7	-22.4	-27.2	-214	9.0	0.0	9.4	0.0	0.0	5.7	0.0	22.9	13.0	56.0
S3	1.1	0.0	0.3	12.9	-1.8	-22.5	-28.2	-219	16.5	0.0	6.8	0.0	0.0	25.8	0.0	67.8	26.1	112.4
S4	2.9	0.1	1.3	10.5	-1.3	-22.5	-33.5	-265	12.1	0.0	24.7	62.5	689.9	12.1	0.0	24.7	62.5	689.9
S5	1.9	0.1	0.7	10.9	-2.4	-21.4	-28.3	-216	7.0	0.0	27.2	11.9	71.4	7.0	0.0	27.2	11.9	71.4
S6	3.0	0.1	1.1	9.6	-0.6	-23.1	-26.8	-208	53.4	0.0	26.0	6.7	37.7	53.4	0.0	26.0	6.7	37.7
S7	2.6	0.2	1.5	8.2	0.9	-20.9	-26.5	-205	18.3	0.3	71.7	42.3	37.5	18.3	0.3	71.7	42.3	37.5
S8	1.3	0.1	0.6	9.1	-2.0	-23.6	-25.9	-194	64.6	0.0	28.9	9.2	33.3	64.6	0.0	28.9	9.2	33.3
S9	5.7	0.3	2.3	9.1	-1.1	-22.3	-24.5	-181	9.5	1.7	30.2	13.5	17.9	9.5	1.7	30.2	13.5	17.9
S10	5.4	0.2	2.3	9.2	0.7	-21.7	-27.2	-200	108.7	0.0	28.1	36.0	33.0	108.7	0.0	28.1	36.0	33.0
S11	6.7	0.3	2.8	9.2	0.8	-21.3	-24.8	-187	14.9	4.0	81.2	35.2	19.4	14.9	4.0	81.2	35.2	19.4
S12	4.9	0.2	2.4	9.7	-0.8	-22.4	-27.4	-211	46.4	0.0	169.7	51.8	41.5	46.4	0.0	169.7	51.8	41.5
S13	6.9	0.3	2.9	9.8	0.4	-20.0	-25.6	-197	40.5	16.4	84.3	31.6	46.0	40.5	16.4	84.3	31.6	46.0
S14	8.0	0.4	3.5	9.9	0.6	-19.7	-27.1	-207	7.9	1.4	41.8	14.1	11.6	7.9	1.4	41.8	14.1	11.6
S15	8.8	0.4	4.1	11.0	0.3	-19.5	-26.3	-201	40.1	16.3	185.9	88.5	56.1	40.1	16.3	185.9	88.5	56.1
S16	6.7	0.3	3.1	10.0	0.3	-20.2	-25.3	-192	23.5	28.7	103.9	65.7	40.2	23.5	28.7	103.9	65.7	40.2
S17	6.6	0.3	2.6	10.0	1.1	-19.8	-24.2	-180	10.5	2.0	27.0	11.8	16.8	10.5	2.0	27.0	11.8	16.8
S18	6.9	0.3	2.6	10.1	0.6	-19.9	-25.3	-193	21.2	11.3	79.1	42.4	26.6	21.2	11.3	79.1	42.4	26.6
S19	7.9	0.3	3.3	10.2	1.1	-20.2	-25.0	-190	22.1	11.5	69.8	38.7	27.4	22.1	11.5	69.8	38.7	27.4
S20	6.0	0.3	3.2	10.4	1.0	-19.7	-25.2	-190	25.2	7.8	59.7	48.4	32.0	25.2	7.8	59.7	48.4	32.0
Mean	4.8	0.2	2.1	9.9	-0.3	-21.2	-26.5	-203	28.9	5.1	58.3	30.5	62.9	28.8	5.1	64.9	33.7	73.7
S.D.	2.6	0.1	1.2	1.0	1.2	1.3	2.0	19	24.9	7.9	49.7	25.0	148.6	25.0	7.9	46.0	22.0	146.9

Figure S1. Phylogenetic relationships among ASV sequences and single-filament PCR sequences obtained in this study. A maximum likelihood tree was constructed using IQ-TREE version 1.6.12 (Nguyen et al., 2015). *Gloeobacter violaceus* PCC 7421 (AF132790.1) was used as an outgroup. Representative sequences identified in this study are shown in bold. "ASV" indicates ASV sequences, and "Single filament PCR" indicates single-filament PCR sequences.

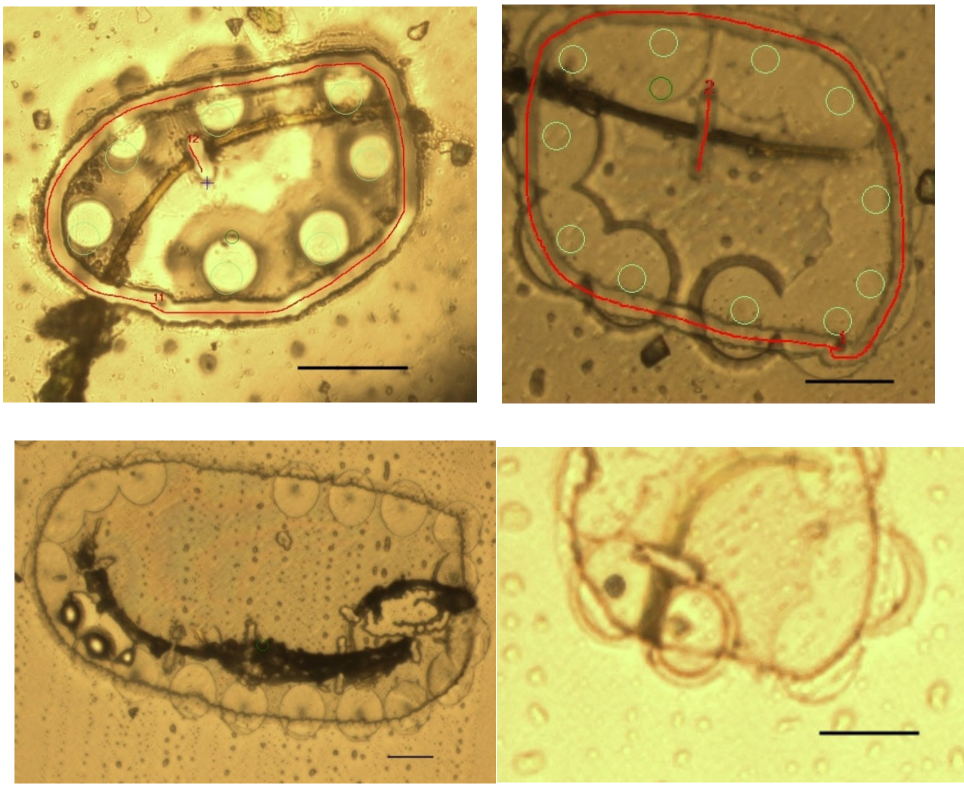

Figure S2: Cyanobacterial cells recovered by single-filament PCR analysis to directly identify the phylotypes comprising cryoconite granules in deeper cryoconite holes. Scale bars represent 50 µm in all images.

ASV ID	OTU ID	Taxonomy	Shallower hole						Deeper hole				Effect size	Wilcoxon p-value	BH-corrected p-value
			S1	S3	S5	S7	S9	S11	S13	S15	S17	S19			
ASV_6	OTU0	Leptolyngbyaceae	0.70	0.75	10.58	4.89	6.25	0	0	0	0	0	1.94	0.0420	0.9699
ASV_21	OTU5	*Pseudanabaena*	2.17	0.97	4.37	1.29	2.73	0.20	0	0.43	0.12	0.07	1.21	0.0225	0.9670
ASV_99	OTU1	*Phormidesmis*	0	0	0.62	1.17	0.22	0.66	0	0.13	0	0	0.64	0.2101	0.9924
ASV_20	OTU2	*Nostoc*	23.29	4.64	0.01	0	0	0	0	0	0	0	0.62	0.3079	0.9901
ASV_0	OTU1	*Phormidesmis*	12.18	7.86	11.49	5.18	2.50	6.94	6.70	3.47	2.94	9.45	0.13	0.7854	0.9950
ASV_28	OTU3	*Chamaesiphon*	0	0	0.88	3.09	2.74	1.21	0.23	1.14	0.34	0.53	0.12	0.5963	1.0000
ASV_42	OTU3	*Chamaesiphon*	0	0	0	0	3.82	0.34	0	0.26	0	0	0.11	0.7342	0.9992
ASV_66	OTU16	Unidentified	0	0	0.20	1.46	0.51	1.27	0.78	0.64	0.15	0	0.02	0.8974	0.9991
ASV_40	OTU16	Unidentified	0	0	0.37	3.42	0.84	2.03	1.35	1.19	0.22	0.48	-0.09	0.7205	0.9929
ASV_76	OTU16	Unidentified	0	0	0.13	0	0.36	0.94	0	0.39	0.49	0.50	-0.29	0.3127	0.9357
ASV_85	OTU7	Leptolyngbyaceae	0	0	0	0.47	0.04	0	0	0.87	0.32	0	-0.40	0.3238	0.9025
ASV_29	OTU16	Unidentified	0	0	0	1.32	1.87	5.45	1.70	1.00	0.64	0.17	-0.44	0.5207	0.9933
ASV_98	OTU3	*Chamaesiphon*	0	0	0	0	0.17	0	0	0.71	0.07	0	-0.52	0.3124	0.8779
ASV_8	OTU16	Unidentified	0	0.04	0.91	4.79	3.33	3.63	5.91	3.68	2.16	3.11	-0.52	0.1245	0.5804
ASV_2	OTU1	*Phormidesmis*	1.55	0.97	1.26	3.80	4.06	3.90	2.83	4.26	1.65	8.97	-0.63	0.2058	0.7518
ASV_1	OTU3	*Chamaesiphon*	0	0	0.70	0.83	2.37	0	5.75	1.94	9.44	2.54	-1.15	0.0075	0.2447
ASV_34	OTU16	Unidentified	0	0	0	0	0.61	1.00	2.52	0.73	1.81	1.51	-1.27	0.0113	0.2947
ASV_106	OTU16	Unidentified	0	0	0	0	0	0	0.69	0.33	0.40	0	-1.39	0.0472	0.4435
ASV_54	OTU16	Unidentified	0	0	0	0	0.17	0.30	2.46	0.73	1.05	0.83	-1.59	0.0000	0.0033
ASV_26	OTU3	*Chamaesiphon*	0	0	0.07	0	0.15	0.12	1.02	1.43	3.58	0.96	-1.72	0.0000	0.0000
ASV_74	OTU16	Unidentified	0	0	0	0	0.33	0	1.32	0.31	0.75	0.74	-1.89	0.0049	0.1864
ASV_5	OTU1	*Phormidesmis*	0	0	0	0	0.05	0.88	6.54	2.25	8.28	5.50	-2.07	0.0000	0.0017

Figure S3: Distribution of the major cyanobacterial ASVs among the samples. The heatmap shows the relative abundance (%) of ASV reads within each sample. The effect size, Wilcoxon p-value, and Benjamini-Hochberg (BH)-corrected p-value, calculated using ALDEx2 to assess the differential abundance between the shallower and deeper holes, are also presented. Absolute effect size ≥ 1 or BH-corrected p-value < 0.1 were colored in red.

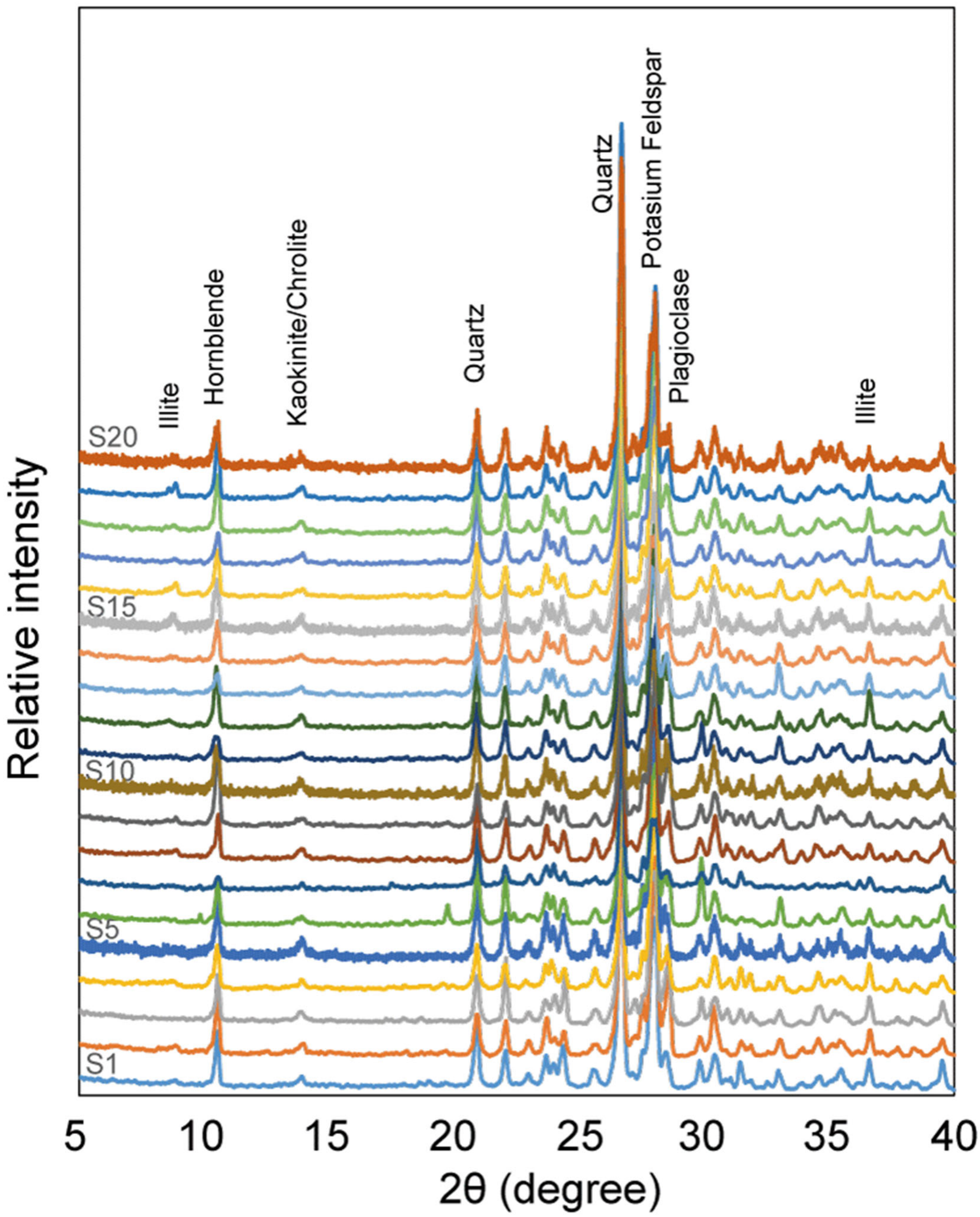

Figure S4: XRD spectra for all samples of cryoconite collected from S1 to S20.

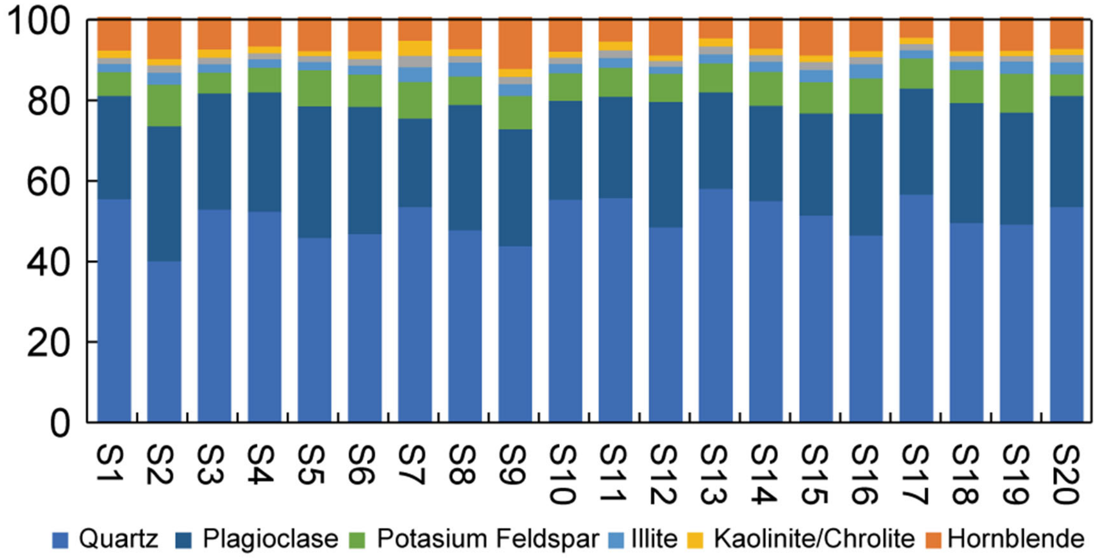

Figure S5: Comparison of the relative peak intensities of minerals in the XRD spectra for all samples of cryoconite collected from S1 to S20.